Inductive Power Transfer for Electric Vehicle Charging – Technical Challenges and Tradeoffs

R. Bosshard,
J. W. Kolar

Inductive Power Transfer for Electric Vehicle Charging

Technical challenges and tradeoffs

by Roman Bosshard and Johann W. Kolar

Increasing public awareness of the environmental impact of greenhouse gas emissions, together with the development of modern lithium-ion batteries, has triggered worldwide interest in electric mobility [1]. Together with environmentally sustainable energy production using renewable energy sources, electric vehicles (EVs) and plug-in hybrid EVs have a smaller CO_2 footprint compared to traditional vehicles that rely exclusively on internal combustion engines. As an additional advantage, the total cost of ownership over the lifetime of an EV is lower than that of a traditional vehicle, despite the higher initial purchase price [2]. Hence, vehicle markets in the developed world have seen EV sales rapidly increasing over the past years.

Nevertheless, further improvement is required to mitigate the technological barriers that currently hinder widespread EV adoption. The development of electrical energy storage systems with ever-higher energy and power densities has already begun to address the limited electrical driving range and long battery-charging time of today's EVs. Still, innovative solutions for battery charging will be required to increase acceptance of the technology and accelerate the transition from traditional to electric mobility. To this end, the miniaturization of isolated conductive on-board EV battery chargers with high power capability is an ongoing research topic: the steady performance improvements are a result of ever-higher converter switching frequencies using novel wide-bandgap power semiconductors [3], soft-switching converter topologies [4], and improved modeling and optimization strategies that allow for the fullest utilization of all system components [5].

Novel Charging Concepts Promote EV Adoption

Novel concepts such as contactless battery charging by inductive power transfer (IPT) [6]–[25] have the potential to further accelerate EV adoption. Unique advantages result from the contactless transmission via IPT of battery-charging energy

across the air gap between a charging platform embedded in the road surface and a receiver coil on the EV. The elimination of the galvanic connection between the charging station and the vehicle simplifies the charging process and removes safety concerns related to the handling of the electrical equipment. In addition, automatic power transfer without the need for moving mechanical components is particularly attractive for charging public transportation EVs because it enables the charging process to be integrated with regular vehicle operation via "opportunity charging" at bus stations, taxicab stands, or traffic lights along the route [25]–[27]. Reduced dwell times for recharging at a depot means that operators can trim the number of vehicles in their fleets and related operating costs.

Further, more frequent recharging reduces the battery's depth of discharge, which extends battery lifetime [28] and allows dimensioning EVs with a smaller on-board energy storage capacity, thus lowering initial costs. Moreover, the lack of a galvanic connection frees the charging station from moving mechanical components, which reduces the required maintenance. These opportunities have triggered a significant number of research projects in industry and in academia around the world (Figure 1). As a result, scientific publications and patent applications on the subject have been increasing rapidly in recent years.

Independent of the employed charging technology, the power electronic components must satisfy multiple performance requirements simultaneously. For low energy costs and simplified thermal management of components, high charging efficiency is required. Moreover, on-board power electronic equipment must meet automotive requirements such as low cost, high reliability, and overall compactness [29], [30]. Another concern is standardization to enable both conductive and contactless EV chargers to interact with products from different manufacturers. For IPT systems, a key interoperability requirement is a common transmission frequency, which will be defined as 85 kHz in the upcoming standard SAE J2954 [31], [32].

In addition to the typical automotive requirements, further design challenges arise for contactless EV chargers as a result of the physical principle of magnetic induction they employ. At higher power levels, high-frequency electromagnetic fields are inherently required for the power transfer. However, if the charger is located in an area accessible by the public, it must comply with the relevant safety standards for electromagnetic fields [33], [34]. Furthermore, the consumer should be confronted with little or no additional effort in using the contactless charger. Hence, the power electronics and the control must have a high tolerance with respect to the coil positioning, such that no particular attention must be paid to the parking position of the EV on the IPT charging platform.

Interdependencies and design tradeoffs exist among the listed performance factors, which, for conventional power electronics, are well documented in the literature

[5]. It was shown in [35] that, for contactless EV chargers, further tradeoffs result from requirements specific to IPT systems. However, a comprehensive investigation of these relations cannot be found in the literature at the present time. Also, a comparison of the attainable performance with existing state-of-the-art conductive EV chargers has not yet been presented. In the meantime, the multiobjective IPT optimization process developed in [35] was applied for the design of a full-scale 50-kW IPT system in [36] and [37]. The technical details of IPT coil optimization and the power electronic converter will be covered in two upcoming papers, [38] and [39], respectively; here, we give only a concise summary of the key results. The main focus of this article is to point
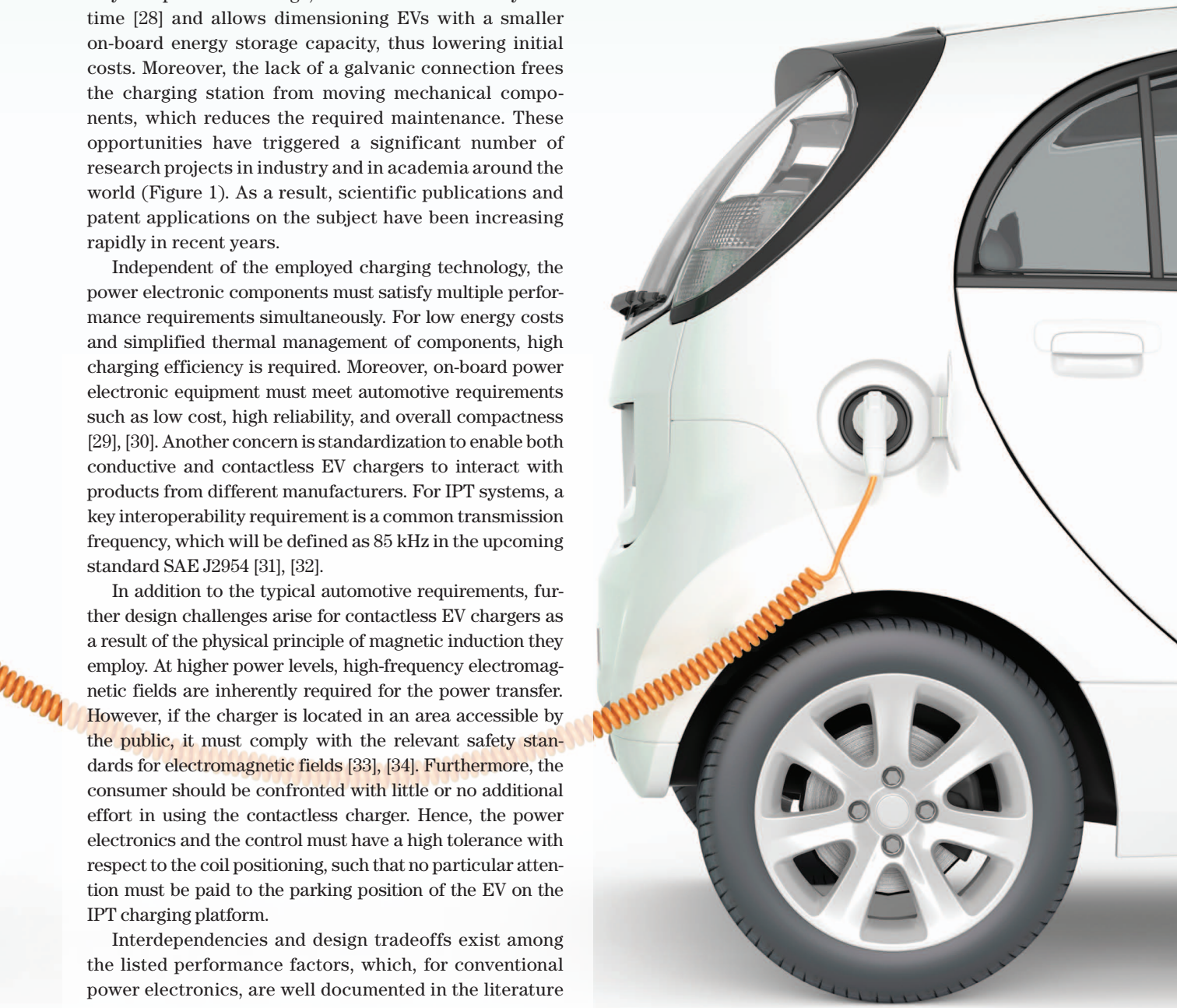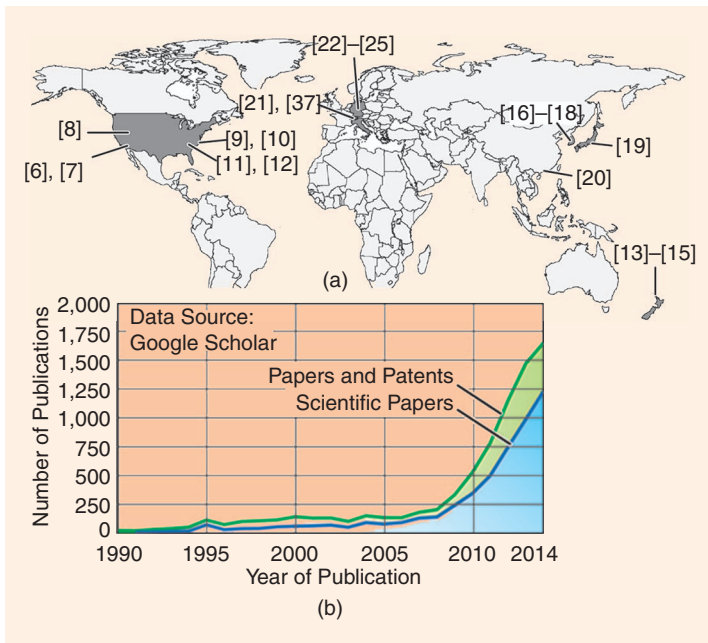
FIG 1 (a) A geographical overview of selected research and development activities on IPT for EV charging. (b) The publication numbers obtained from the following Google Scholar search query: *power inductive OR contactless "electric vehicle"–"induction motor"–"induction machine."* (The last two parts exclude electrical machine research with similar titles.)

out the limitations of IPT technology for EV charging as compared to conventional conductive chargers, based on the theoretical and experimental results obtained from the 50-kW prototype. For the sake of brevity, the observations are presented as a high-level discussion without considering all the technical details, for which interested readers are referred to [36]–[40].

Figure of Merit for IPT Systems

Based on the theoretical analysis of the transformer equivalent circuit of a series–series compensated IPT system, it was shown in [41]–[43] that the figure of merit FOM = kQ limits the transmission (or coil-to-coil) efficiency to

$$\eta_{\max} \approx 1 - \frac{2}{kQ}, \qquad (1)$$

where k represents the magnetic coupling and Q the quality factor of the two IPT coils at the operating frequency ω_0. The magnetic coupling accounts for the magnetizing current [compare i_μ in Figure 2(b)] that is necessary to sustain a certain power output P_{out}, while the quality factor represents the ac power losses P_{loss} that occur in the coil windings as a result of the parasitic resistance of the copper litz wire conductors.

The magnetic coupling is mainly a function of the ratio between the air gap and the size of the IPT coils, as shown in Figure 2(c) for an exemplary configuration. Hence, larger IPT coils lead to higher efficiency for a given transmission distance. In addition, the magnetic coupling decreases rapidly with misaligned IPT coils. Therefore, large IPT coils are needed to limit the variation of the magnetic coupling and to achieve a sufficient misalignment tolerance. If, as a first approximation, the ac effects in the litz wire windings and the losses in the magnetic core elements are neglected, the quality factor $Q \approx \omega_0 L / R_{\mathrm{ac}}$ is proportional to the transmission frequency [Figure 2(d)]. In addition, the quality factor also increases with the coil size because of the increasing inductance that results from the larger coil area enclosed by the windings. Hence, the transmission efficiency is defined by the size of the IPT coils as compared to the air gap and by the selected transmission frequency.

For a given area-related power density $\alpha = P_{\mathrm{out}} / A_{\mathrm{coil}}$ of the IPT coils and assuming natural convection cooling, the coil surface-related power loss density is thermally limited to $P_{\mathrm{surf,max}} = P_{\mathrm{loss,max}} / A_{\mathrm{coil}}$ by the heat transfer coefficient at the coil surface and the IPT coil surface area A_{coil}. This thermal limit defines a required minimum efficiency of

$$\eta_{\min} \approx 1 - \frac{P_{\mathrm{loss,max}}}{P_{\mathrm{out}}} = 1 - \frac{P_{\mathrm{surf,max}}}{\alpha} \quad (2)$$

and, thereby, a required minimum coil size for the dissipation of the power losses $P_{\mathrm{loss,max}}$ that result during the transfer of a given charging power P_{out}. Depending on the materials used for the coil housing and on the power level,
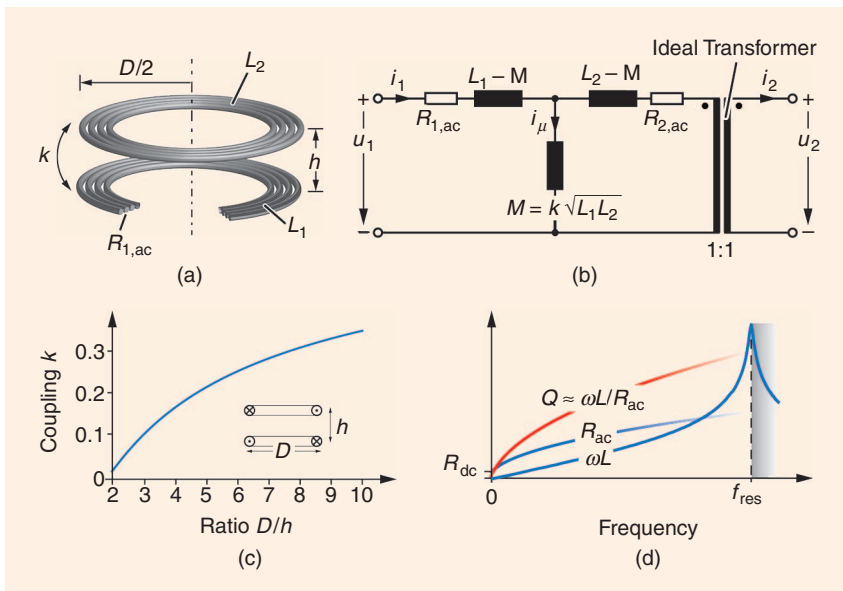

FIG 2 (a) A four-turn spiral air coil pair. (b) A transformer equivalent circuit. (c) The calculated magnetic coupling as a function of the ratio of the coil diameter to the air gap. (d) The approximate frequency dependency of the coil impedances and the quality factor.

the minimum coil size can be large compared to the air gap distance. For more compact IPT coils with a smaller surface area, active cooling is needed for the thermal management.

Note that a design tradeoff among the coil size, the transmission efficiency, and the stray field exists for IPT systems. According to Faraday's law, the induced voltage in the receiver coil is proportional to the magnetic flux in the air gap, the area enclosed by the windings, and the transmission frequency. Assuming a fixed observation point, IPT coils with larger physical dimensions result in higher magnetic fields. Even though the transmitter current is lower for larger coils with improved magnetic coupling, the close proximity of the conductors to the observation point leads to an increase in the magnetic field. Therefore, the remaining option for reducing the necessary magnetic fields in an IPT system is to select a higher transmission frequency. However, the high transmission frequency poses a challenge for the power electronics design. In the next section, these tradeoffs are investigated more closely for the IPT system [37], with the goal of accurately quantifying the performance limits for a specific system configuration.

> *A design tradeoff between the coil size, the transmission efficiency, and the stray field exists for IPT systems.*

the regulation of the power flow in the series–series compensated IPT system, the dc-link voltages $U_{1,dc}$ and $U_{2,dc}$ at the transmitter and at the receiver are actively controlled. For the dc–dc converter on the vehicle, a parallel-interleaved modular approach with coupled magnetic components is chosen for maximum compactness of the power electronics. At the transmitter side, the control of the dc-link voltage is provided by a buck-and-boost-type three-phase mains interface [44], [45]. A coordinated feedback control of both dc-link voltages via a wireless communication link allows regulation of the battery-charging current at the converter output in an efficient and robust manner over a wide load range [37].

The results of the multiobjective optimization of the transmission coils are summarized in Figure 4(b) and (c). Each point represents the calculated performance of a different IPT coil design. Included are the ac winding losses, core losses, and eddy-current shielding losses in the coils, as well as the losses in the film capacitors used for the employed compensation. For coils with a high area-related power density α, the magnetic coupling k is lower because of the smaller coil area [compare the coloring in Figure 4(b)]. Thus, the

The Design Tradeoffs for Contactless Chargers

For the design of the 50-kW/85-kHz IPT system shown in Figure 3, the multiobjective optimization process proposed in [35] was adopted. As illustrated in Figure 4(a), mathematical models describing the physical properties and the system operation (power losses, component dimensions, system cost, topology, modulation, etc.) are used to iteratively calculate the performance of all system configurations contained in a specified design space. The core elements of the method are the comprehensive component and system models, which are based on a combination of analytical models and three-dimensional finite-element-method calculations, as described in full detail in [37] and [38]. Here, only a short overview of the system architecture is given, and the main optimization results are summarized.

The topology of the contactless EV charger and the realized prototype hardware are shown in Figure 3. For
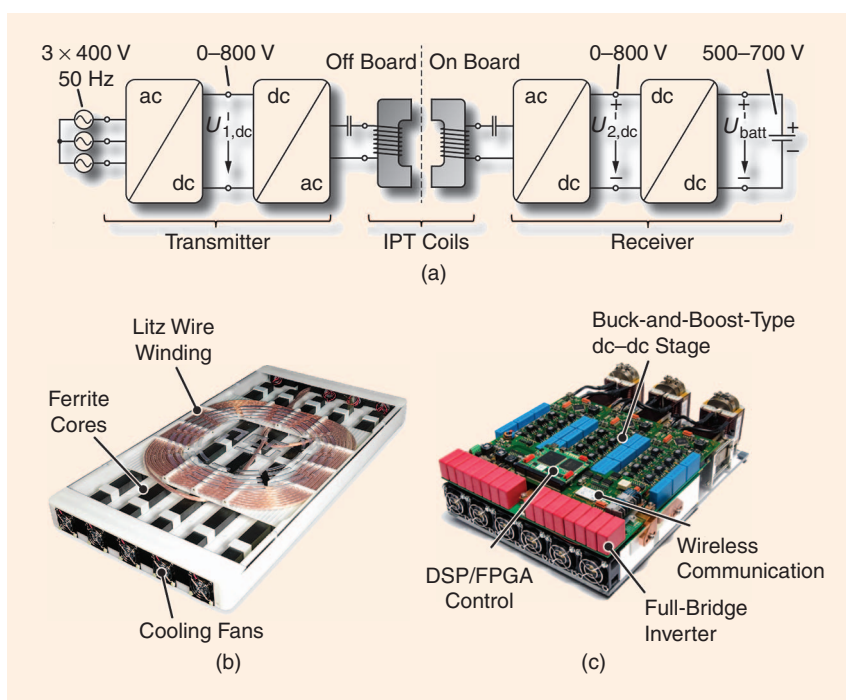

FIG 3 (a) An IPT system power-conversion chain from the three-phase mains to the EV high-voltage battery. (b) A 50-kW IPT coil with a transmission efficiency of 98%, an area-related power density of 1.6 kW/dm^2, and a gravimetric power density of 2.0 kW/kg (including all passive materials and cooling system). (c) An all-SiC vehicle-side power converter with a dc-to-ac efficiency of 98.6% and a power density of 9.5 kW/dm^3. DSP: digital signal processor; FPGA: field-programmable gate array.
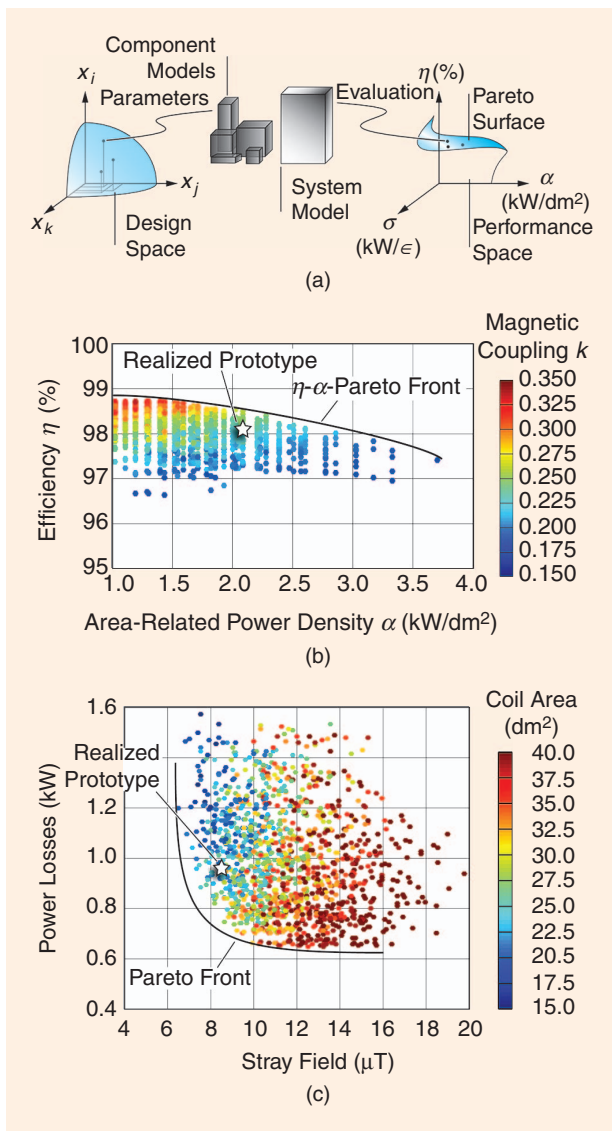
FIG 4 (a) The multiobjective power electronics optimization: component and system models map the system parameters of the design space onto the performance space, where a multidimensional Pareto surface limits the performance of the technology. The results of the multiobjective IPT coil optimization: (b) the transmission efficiency η of a forced-air cooled $P_{out} = 50$-kW system with an air gap of 160 mm and a resonant frequency of 85 kHz as a function of the area-related power density $\alpha = P_{out}/A_{coil}$; (c) the tradeoff between the total coil losses and the magnetic stray field at 1.10-m distance from the coil center.

transmission efficiency η is reduced as expected from (1). In return, a smaller amount of active materials is required for the more compact IPT coils, which results in a lower coil weight and reduced material costs. At the performance limit, the area-related power density α can be increased only at the price of a lower transmission efficiency η. This design tradeoff is described by the η-α-Pareto front.

Not captured by this analysis is the fact that the magnetic coupling and therefore the transmission efficiency

of smaller coils become more sensitive to the positioning of the EV. Only an overdimensioning of the transmitter coil and the power electronics or the use of an array of multiple, selectively activated transmitters can provide sufficient coil-misalignment tolerance. Consequently, there also exists a tradeoff between the coil size, the complexity of the transmitter, and the positioning tolerance.

A low magnetic stray field presents the third key performance factor for a contactless EV charger. The IPT system must comply with the relevant safety standards for the magnetic field [31], [33], [34] in all regions that are accessible to humans, i.e., in the passenger cabin and at all sides of the vehicle. Because the passenger cabin is shielded by the EV's metallic chassis, the main concern is the stray field around the vehicle. In practice, the magnetic field would be measured with a field probe at test locations within this area, at a fixed distance from the EV specified by a standard.

For the multiobjective optimization of the 50-kW/85-kHz IPT system, the influence of the EV chassis is not included in the sense of a worst-case analysis. In the compliance test measurements, the magnetic stray field is sampled at a fixed distance of 1.10 m from the coil center (the critical distance in the industry application at hand), assuming that the IPT coil is mounted centrally below the EV. The obtained results are shown in Figure 4(c). On the indicated Pareto front, the stray field can be reduced only if the IPT coils, i.e., the magnetic field source, are made smaller to increase the distance from the current-carrying conductors to the observation point [compare the coloring in Figure 4(c)]. However, the smaller IPT coils lead to a lower magnetic coupling and a reduced transmission efficiency. Therefore, a design tradeoff results among the magnetic stray field, the coil size, and the power losses. To overcome this limit, additional shielding of the IPT coils must be implemented, at the cost of additional system complexity.

The presented results do not include the power electronic converter, from which additional volume, weight, and cost arise. At higher power levels, off-board conductive dc chargers are typically connected to the vehicle at the receiver-side dc link [compare $U_{2,dc}$ in Figure 3(a)] for minimizing the number of on-board power conversion stages. For the contactless charger, a larger fraction of the power electronics must be located on the vehicle due to the intrinsic division of the system at the air gap between the IPT coils. In addition, controlling power transfer with high efficiency over a wide load range requires a comparably high level of complexity. Significant simplifications typically lead to lower efficiency and, consequently, higher energy cost for the EV charger, e.g., caused by switching losses in the power converter [24]. Thus, for the on-board power electronics of a high-power contactless charger, a higher volume, weight, and cost are expected than for an off-board conductive dc charger. The effort for the vehicle-side

Table 1. An overview of state-of-the-art conductive and contactless EV chargers.

	Source	P (kW)	V (dm³)	m (kg)	η (%)	ρ (kW/dm³)	γ (kW/kg)
Conductive	m-pec[1] [www.mpec.at]	6.6	1.38	2.53	96.0	4.8	2.6
	Whitaker[2] et al. [3]	6.1	1.22	1.6	95.0	5.0	3.8
	J. Everts [46]	3.7	1.85	2.68	95.6	2.0	1.38
	Gautam et al. [47]	3.3	5.46	6.2	93.6	0.60	0.53
	GM Chevrolet Volt [12]	3.3	6.71	10.1	89.6	0.49	0.33
	Nissan Leaf 2013 [48]	3.3	10.9	16.3	85	0.3	0.2
	Toyota Prius 2010 [3]	2.9	6.4	6.6	n/a	0.45	0.44
Contactless	Primove 200[3, 4] [25]	200	198	340	90.0	1.0	0.59
	Bosshard[5] et al. [37], [38]	50	18.5	25	95.8	2.7	2.0
	Goeldi[5] et al. [23]	22	22.4	n/a	97.0	0.98	n/a
	Chinthavali et al. [12]	6.6	7.2	12.3	85.0	0.92	0.54
	Brusa ICS115[3] [21]	3.7	2.3	4.0	90.0	1.60	0.93
	WiTricity WiT3300[3] [10]	3.3	1.8	4.0	89.0	1.83	0.83
	Diekhans[5, 6] et al. [24]	3.0	8.5	3.2	95.8	0.35	0.93

Remarks: For all contactless chargers, only the dimensions and weight of the receiver coil are included. [1]Designed with Si CoolMOS devices. [2]Designed with SiC MOSFET devices. [3]Data obtained from manufacturer upon request. [4]The receiver is lowered to the street during charging. [5]DC-to-dc efficiency. [6]No coil housing included.

IPT power electronics is closer to that of a conductive on-board charger, given the similarity of the power-conversion chains; see Figure 3(a) and [3].

For passenger EVs, a contactless system could be considered as an optional premium feature in addition to a conventional conductive charger. In this case, integration of the two on-board power converters reduces the required constructive volume and the total cost for the charging equipment. However, the major volume, weight, and cost increase due to the receiver coil remains, despite the combination of the power electronics.

The State of the Art for Conductive and Contactless EV Chargers

The presented analysis indicates that the required component volume, weight, and material costs for the IPT on-board components are higher than for a conventional solution. This is confirmed by the data of existing on-board conductive EV chargers collected in Table 1. The listed numbers for the conductive chargers include the complete power-conversion chain from the mains to the EV high-voltage battery. For the contactless chargers, only the receiver coil is included for the volumetric and gravimetric power density. Data for industry prototype IPT chargers [10], [21], [25] are compared in Figure 5. For completeness, the results for the 50-kW/85-kHz IPT system in [37] are also included. It must be pointed out that the listed commercial systems include structural elements for mounting the coil on the vehicle and comply with automotive standards. For the work in [37], further modifications are required to fulfill all automotive requirements. As a comparison, the best-in-class 6.1-kW conductive EV charger described in [3] is also shown.
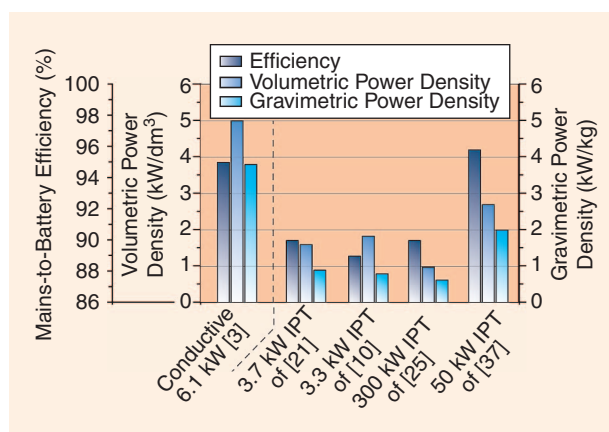

FIG 5 A comparison of the main performance factors for a conductive on-board EV charger, for industrially available IPT chargers, and for the system presented in this work. The power density for the IPT systems includes only the receiver coil, whereas for [3] the complete system is included.

The listed data highlight that the efficiency of the contactless EV chargers is reduced by approximately 5% compared to the latest conductive EV chargers. This is mainly due to the limited construction volume for the receiver coil on the vehicle. Small receiver coils lead to a low magnetic coupling even if, as in [21], a significantly larger transmitter coil is used. As a result, a comparably low transmission efficiency must be accepted for a contactless EV charger.

The outstanding performance of the conductive charger in [3] is achieved by the optimum utilization of silicon carbide (SiC) power-semiconductor technology and a high switching frequency for the miniaturization of the passive
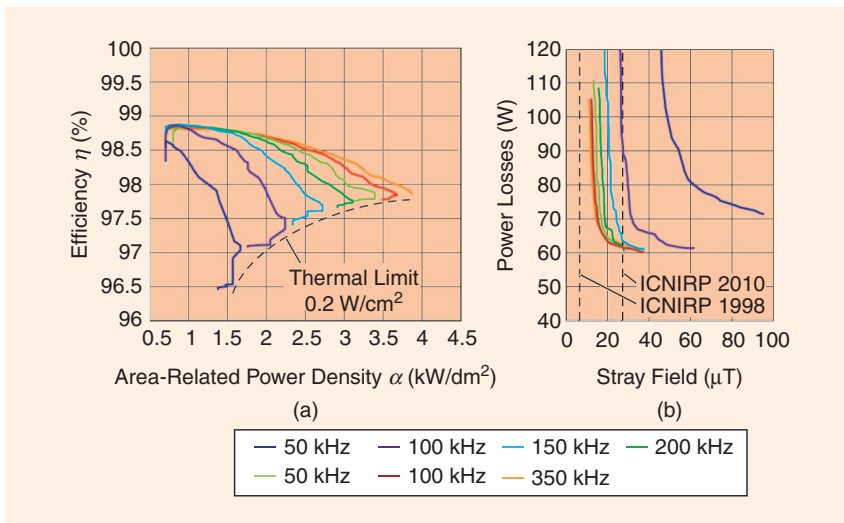
FIG 6 (a) The η-α-Pareto fronts and (b) the tradeoff between coil losses and the stray field of a scaled 5-kW prototype IPT system, calculated for optimum loading conditions of the resonant circuit and different transmission frequencies between 50 and 350 kHz. (Figure reproduced from [35].) ICNIRP: International Commission on Non-Ionizing Radiation Protection.

components. For a contactless charger, this is possible only to a limited extent. A reduction in coil size is always tied to the tradeoff in terms of transmission efficiency. The increasing power losses due to the low magnetic coupling and the difficulty of cooling the IPT coils without eddy-current-prone metal heat sinks restrict the use of small coils at a high power level.

Future Perspectives for IPT

The previously discussed design tradeoffs represent technology barriers that cannot be crossed using the considered power electronics topology, IPT coil geometry, and materials. They can be extended only by technological progress (digital control, wide-bandgap power semiconductors, etc.) or by novel concepts with inherently superior performance [5].
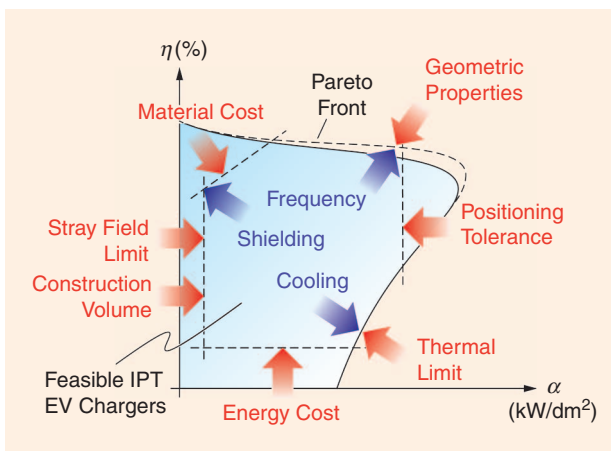

FIG 7 A schematic representation of the feasible performance space of contactless EV chargers based on IPT, including the effects of the technological constraints and potential ways for future improvement.

For the passive materials of the IPT coils, a large technological step is currently not in sight. Litz wire, ferrite, and film capacitors are components with a long-established quality and little room for improvement. Some advantages could result from novel synthetic materials for the coil housing. Enclosure of the IPT coil in thermally conductive polymer or epoxy resin could simplify the thermal management. However, a disruptive technology improvement seems unlikely at the present time.

The design parameter with the highest potential for crossing the barriers is the transmission frequency. Figure 6 shows the η-α-Pareto fronts and the design tradeoff for the stray field for a scaled 5-kW laboratory prototype designed in [35]. At an increased transmission frequency, the efficiency of the power transfer is higher for the same power density, and reduced magnetic stray fields are possible. Additional research is still needed to quantify the attainable increase in efficiency and power density if the power converters are also included. However, decreasing advantages are expected at a sufficiently high frequency as a result of the frequency-dependent losses in the power electronics and the core materials. In addition, the power electronics design becomes more and more challenging due to the impact of the parasitic elements of the IPT coils and the converter. In addition, the upcoming interoperability standard SAE J2954 sets the transmission frequency as 85 kHz, which effectively blocks development in this direction.

Further technological limitations result from the electromagnetic fields that are inherently required by the employed physical principle. When increasing the power level of a contactless EV charger, the stray fields become a limiting factor, and extensive shielding is necessary. Especially for the high transmission frequencies achieved with novel fast-switching wide-bandgap power semiconductors, electromagnetic compliance filtering for IPT systems is also needed specifically to limit the electric stray field. Future developments in this field, therefore, could help overcome technological barriers.

Considering these barriers, the outlook for significant improvements is limited for IPT systems, as the size, weight, and material cost for the receiver coil are restricted by design tradeoffs that foreseeable technological advances are unlikely to change.

Conclusions

The analysis presented here of the design tradeoffs of IPT systems compared to existing state-of-the-art EV chargers highlights that realization of a compact

contactless charger poses a major design challenge. On the one hand, a drastic drop in efficiency, the challenging thermal management of the IPT coils, and an inferior coil positioning tolerance restrict an increase of the power density (Figure 7). On the other hand, small coils are required to limit the necessary construction volume and material cost of the vehicle-side components, as well as to minimize the magnetic stray field of IPT systems. Elevating the transmission frequency can increase the efficiency of high-power-density coil designs, while at the same time reducing the magnetic stray field. However, the approach is limited by increasing losses in the power electronics, and it has recently been rendered unattractive by the specification of 85 kHz as a common frequency in SAE J2954.

For a conductive EV charger, the converter switching frequency can be freely selected for design optimizations, e.g., for the miniaturization of the passive components. In addition, the converter topology and the high-frequency isolation transformer can be optimized irrespective of the geometric arrangement in the application itself. Hence, this technology can fully benefit from technological progress, e.g., from the steady improvement of wide-bandgap power semiconductors. This means that future performance improvements and material cost reductions may be anticipated. In stark contrast, for IPT systems the attainable performance is governed mainly by the geometric properties of the application and by the physics that describe the transmission coil system. Therefore, the perspective for future improvements is limited for contactless EV charging.

Nevertheless, contactless EV charging remains an attractive solution if the lower efficiency and the increased on-board component volume are acceptable for the application at hand. IPT offers the unique advantage of a galvanically isolated power transfer to the vehicle without the need for moving mechanical parts that are subject to corrosion, wear, and fatigue. This is highly attractive for the opportunity charging of public transport systems, where the reliability and the maintenance requirements of the charger are a considerable factor in the operating costs. For passenger EVs, a contactless charger with a lower power level, e.g., 3–7 kW, and therefore a smaller size could be considered as a premium feature in addition to a high-power conductive charger rated for 22 kW or more. To reduce the cost and limit the necessary construction volume on the vehicle, the on-board power electronics of both charging systems could be optimally integrated into a single unit. In this way, the contactless charger would improve the convenience and safety for the routine use case, while faster battery recharging would remain possible with the conductive charger.

Acknowledgment

About the Authors
Roman Bosshard (bosshard@lem.ee.ethz.ch) is with ABB Switzerland, Turgi. Formerly, he was with the Power Electronic Systems Laboratory, ETH Zurich, Switzerland. He is a Student Member of the IEEE.

Johann W. Kolar (kolar@lem.ee.ethz.ch) is a full professor and the head of the Power Electronic Systems Laboratory at ETH Zurich, Switzerland. He is a Fellow of the IEEE.

References
[1] T. Trigg. (2012, spring). The third age of electric vehicles. *J. Int. Energy Agency.* [Online]. 2, pp. 30–31. Available: http://www.iea.org/media/images/Issue2_Evs.pdf

[2] International Energy Agency. (2013, Apr.). Global EV outlook: Understanding the electric vehicle landscape to 2020. [Online]. Available: https://www.iea.org/publications/freepublications/publication/GlobalEV-Outlook_2013.pdf

[3] B. Whitaker, A. Barkley, Z. Cole, B. Passmore, D. Martin, T. McNutt, A. Lostetter, J. S. Lee, and K. Shiozaki, "A high-density, high-efficiency, isolated on-board vehicle battery charger utilizing silicon carbide power devices," *IEEE Trans. Power Electron.*, vol. 29, no. 5, pp. 2606–2617, Mar. 2014.

[4] I. Jitaru, "A 3 kW soft switching DC-DC converter," in *Proc. 15th Applied Power Electronics Conf. Exposition*, New Orleans, LA, Feb. 2000, pp. 86–92.

[5] J. W. Kolar, J. Biela, S. Waffler, T. Friedli, and U. Badstübner, "Performance trends and limitations of power electronic systems," in *Proc. Sixth Int. Conf. Integrated Power Electronics Systems*, Nuremberg, Germany, Mar. 2010, pp. 1–20.

[6] J. Bolger, F. Kirsten, and L. Ng, "Inductive power coupling for an electric highway system," in *Proc. 28th Vehicular Technology Conf.*, vol. 28, Denver, CO, Mar. 1978, pp. 137–144.

[7] K. Lashkari, S. E. Schladover, and E. H. Lechner, "Inductive power transfer to an electric vehicle," in *Proc. Eighth Int. Electric Vehicle Symp.*, Washington, D.C., Oct. 1986.

[8] Wave IPT. Wirelessly charging electric vehicles. [Online]. Available: www.waveipt.com

[9] A. Kurs, A. Karalis, R. Moffatt, J. D. Joannopoulos, P. Fisher, and M. Soljačić, "Wireless power transfer via strongly coupled magnetic resonances," *Science*, vol. 317, no. 5834, pp. 83–86, 2007.

[10] WiTricity Corp. (2014). WiT-3300 resonator pair R2.3 (data sheet). [Online]. Available: http://www.witricity.com/assets/WiT-3300_R2.3_DS.pdf

[11] O. C. Onar, J. M. Miller, S. L. Campbell, C. Coomer, C. P. White, and L. E. Seiber, "Oak Ridge National Laboratory wireless power transfer development for sustainable campus initiative," in *Proc. IEEE Transportation Electrification Conf. Expo.*, Detroit, MI, June 2013, pp. 1–8.

[12] M. Chinthavali, O. C. Onar, S. L. Campbell, and L. M. Tolbert, "Integrated charger with wireless charging and boost functions for PHEV and EV applications," in *Proc. IEEE Transportation Electrification Conf. Expo.*, Dearborn, MI, June 2015, pp. 1–8.

[13] A. W. Green and J. T. Boys, "10 kHz inductively coupled power transfer-concept and control," in *Proc. Fifth Int. Conf. Power Electron. Variable-Speed Drives*, London, U.K., Oct. 1994, pp. 694–699.

[14] M. Budhia, J. Boys, G. Covic, and C. Y. Huang, "Development of a single-sided flux magnetic coupler for electric vehicle IPT charging systems," *IEEE Trans. Ind. Electron.*, vol. 60, no. 1, pp. 318–328, Jan. 2013.

[15] G. Covic and J. Boys, "Inductive power transfer," *Proc. IEEE*, vol. 101, no. 6, pp. 1276–1289, June 2013.

[16] J. Kim, J. Kim, S. Kong, H. Kim, I. S. Suh, N. P. Suh, D. H. Cho, J. Kim, and S. Ahn, "Coil design and shielding methods for a magnetic resonant wireless power transfer system," *Proc. IEEE*, vol. 101, no. 6, pp. 1332–1342, June 2013.

[17] S. Choi, B. Gu, S. Jeong, and C. Rim, "Advances in wireless power transfer systems for roadway-powered electric vehicles," *IEEE J. Emerg. Select. Topics Power Electron.*, vol. 3, no. 1, pp. 18–36, 2015.

[18] S. Y. Choi and C. T. Rim, "Recent progress in developments of on-line electric vehicles," in *Proc. First Int. Conf. Power Electronics Systems Applications*, Hong Kong, Dec. 2015, pp. 1–8.

[19] Toyota Motor Corp. (2014, Feb. 13). Toyota to begin wireless vehicle charging verification testing. [Online]. Available: http://newsroom.toyota.co.jp/en/detail/651273

[20] S. Y. R. Hui, W. X. Zhong, and C. K. Lee, "A critical review of recent progress in mid-range wireless power transfer," *IEEE Trans. Power Electron.*, vol. 29, no. 9, pp. 4500–4511, Sept. 2014.

[21] Brusa Elektronik AG. (2014). Inductive charging system ICS115 (data sheet). [Online]. Available: http://www.brusa.biz/en/products/charger/inductive-charging/ics115.html

[22] Conductix Wampfler/Delachaux SA. (2012, May 31). 10 years of electric buses with IPT charge. [Online]. Available: http://www.conductix.us/en/news/2012-05-31/10-years-electric-buses-iptr-charge

[23] B. Goeldi, S. Reichert, and J. Tritschler, "Design and dimensioning of a highly efficient 22 kW bidirectional inductive charger for e-mobility," in *Proc. Int. Exhibition Conf. Power Electronics*, Nuremberg, Germany, 2013, pp. 1496–1503.

[24] T. Diekhans and R. De Doncker, "A dual-side controlled inductive power transfer system optimized for large coupling factor variations and partial load," *IEEE Trans. Power Electron.*, vol. 30, no. 11, pp. 6320–6328, Nov. 2015.

[25] Bombardier Transportation. (2013). Primove: Introducing true electric mobility for a sustainable future. [Online]. Available: http://primove.bombardier.com/fileadmin/primove/content/MEDIA/Publications/BT_Brochure_PRIMOVE_210x280_2013_final_upd_110dpi_SP.pdf

[26] B. Warner, O. Augé, and A. Moglestue. (2013, Apr.) Taking charge: Flash charging is just the ticket for clean transportation. *ABB Rev.* [Online]. Available: https://library.e.abb.com/public/ba824879a3b6dd2ec1257c5a0041be95/64-69%204m341_EN_72dpi.pdf

[27] Siemens AG. (2015). Charge your future—with the Siemens eBus charging infrastructure. [Online]. Available: http://w3.siemens.com/topics/global/de/elektromobilitaet/PublishingImages/ladetechnik-busse/pdf/ebus-charge-your-future-en.pdf

[28] D. Magnor, J. B. Gerschler, M. Ecker, P. Merk, and D. U. Sauer, "Concept of a battery aging model for lithium-ion batteries considering the lifetime dependency on the operation strategy," in *Proc. 24th European Photovoltaic Solar Energy Conf.*, Hamburg, Germany, Sept. 2009, pp. 3128 – 3134.

[29] M. März, A. Schletz, B. Eckardt, S. Egelkraut, and H. Rauh, "Power electronics system integration for electric and hybrid vehicles," in *Proc. Sixth Int. Conf. Integrated Power Electronics Systems*, Nuremberg, Germany, Mar. 2010, pp. 1–10.

[30] M. Yilmaz and P. Krein, "Review of battery charger topologies, charging power levels, and infrastructure for plug-in electric and hybrid vehicles," *IEEE Trans. Power Electron.*, vol. 28, no. 5, pp. 2151–2169, May 2013.

[31] Society of Automotive Engineers. (2016). Wireless power transfer for light-duty plug-in/electric vehicles and alignment methodology. [Online]. SAE Std. J2954 (unpublished). Available: http://standards.sae.org/wip/j2954/

[32] Society of Automotive Engineers. (2013). SAE international task force announces agreement on frequency of operation and power classes for wireless power transfer for its electric and plug-in electric vehicle guideline (press release). [Online]. Available: http://www.sae.org/servlets/pressRoom?OBJECT_TYPE=PressReleases&PAGE=showRelease&RELEASE_ID=2296

[33] International Commission on Non-Ionizing Radiation Protection (ICNIRP), "Guidelines for limiting exposure to time-varying electric and magnetic fields (1 Hz to 100 kHz)," *Health Phys.*, vol. 99, no. 6, pp. 818–836, 2010.

[34] *IEEE Standard for Safety Levels with Respect to Human Exposure to Radio Frequency Electromagnetic Fields, 3 kHz to 300 GHz*, IEEE International Committee on Electromagnetic Safety Standard C95.1, 2005.

[35] R. Bosshard, J. W. Kolar, J. Mühlethaler, I. Stevanović, B. Wunsch, and F. Canales, "Modeling and η-α-Pareto optimization of inductive power transfer coils for electric vehicles," *IEEE J. Emerg. Select. Topics Power Electron.*, vol. 3, no. 1, pp. 50–64, Mar. 2015.

[36] R. Bosshard and J. W. Kolar, "Fundamentals and multi-objective design of inductive power transfer systems (Tutorial)," in *Proc. 17th European Conf. Power Electronics Applications (EPE-ECCE Europe)*, Geneva, Switzerland, Sept. 2015.

[37] R. Bosshard, "Multi-objective optimization of inductive power transfer systems for EV charging," Ph.D. dissertation, ETH Zurich, Switzerland, 2015.

[38] R. Bosshard and J. W. Kolar, "Multi-objective optimization of 50 kW/85 kHz IPT system for public transport," *IEEE J. Select. Eng. Topics in Power Electron.*, early access, 2016.

[39] R. Bosshard and J. W. Kolar, "All-SiC 9.5 kW/dm3 on-board power electronics for 50 kW/85 kHz automotive IPT system," unpublished, 2016.

[40] R. Bosshard, U. Iruretagoyena, and J. W. Kolar, "Comprehensive evaluation of rectangular and double-d coil geometry for 50 kW/85 kHz IPT system," *IEEE J. Select. Eng. Topics in Power Electron.*, early access, 2016.

[41] J. C. Schuder, "Powering an artificial heart: Birth of the inductively coupled-radio frequency system in 1960," *Artificial Organs*, vol. 26, no. 11, pp. 909–915, June 2002.

[42] K. van Schuylenbergh and R. Puers, *Inductive Powering: Basic Theory and Application to Biomedical Systems*. Dordrecht, The Netherlands: Springer, 2009.

[43] E. Waffenschmidt and T. Staring, "Limitation of inductive power transfer for consumer applications," in *Proc. 13th Euro. Conf. Power Electronics Applications (EPE-ECCE Europe)*, Barcelona, Spain, Sept. 2009, pp. 1–10.

[44] T. Nussbaumer, M. Baumann, and J. W. Kolar, "Comprehensive design of a three-phase three-switch buck-type PWM rectifier," *IEEE Trans. Power Electron.*, vol. 22, no. 2, pp. 551–562, Mar. 2007.

[45] T. Friedli, M. Hartmann, and J. W. Kolar, "The essence of three-phase PFC rectifier systems—Part II," *IEEE Trans. Power Electron.*, vol. 29, no. 2, pp. 543–560, Feb. 2014.

[46] J. Everts, "Modeling and optimization of bidirectional dual active bridge DC-DC converter topologies," Ph.D. dissertation, Univ. (KU) Leuven, Belgium, 2014.

[47] D. Gautam, F. Musavi, M. Edington, W. Eberle, and W. Dunford, "An automotive onboard 3.3-kW battery charger for PHEV application," *IEEE Trans. Veh. Technol.*, vol. 61, no. 8, pp. 3466–3474, Oct. 2012.

[48] T. Burress (2015, June 9). Benchmarking EV and HEV technologies. [Online]. Available: http://energy.gov/sites/prod/files/2015/06/f24/edt006_burress_2015_o.pdf